

ARMY RESEARCH LABORATORY



Millimeter-Wave Propagation Measurement Through a Dust Tunnel

by David Wikner

ARL-TR-4399

March 2008

NOTICES

Disclaimers

The findings in this report are not to be construed as an official Department of the Army position unless so designated by other authorized documents.

Citation of manufacturer's or trade names does not constitute an official endorsement or approval of the use thereof.

Destroy this report when it is no longer needed. Do not return it to the originator.

Army Research Laboratory

Adelphi, MD 20783-1197

ARL-TR-4399

March 2008

Millimeter-Wave Propagation Measurement Through a Dust Tunnel

David Wikner

Sensors and Electron Devices Directorate, ARL

REPORT DOCUMENTATION PAGE

Form Approved
OMB No. 0704-0188

Public reporting burden for this collection of information is estimated to average 1 hour per response, including the time for reviewing instructions, searching existing data sources, gathering and maintaining the data needed, and completing and reviewing the collection information. Send comments regarding this burden estimate or any other aspect of this collection of information, including suggestions for reducing the burden, to Department of Defense, Washington Headquarters Services, Directorate for Information Operations and Reports (0704-0188), 1215 Jefferson Davis Highway, Suite 1204, Arlington, VA 22202-4302. Respondents should be aware that notwithstanding any other provision of law, no person shall be subject to any penalty for failing to comply with a collection of information if it does not display a currently valid OMB control number.

PLEASE DO NOT RETURN YOUR FORM TO THE ABOVE ADDRESS.

1. REPORT DATE (DD-MM-YYYY) March 2008		2. REPORT TYPE Final		3. DATES COVERED (From - To)	
4. TITLE AND SUBTITLE Millimeter-Wave Propagation Measurement Through a Dust Tunnel				5a. CONTRACT NUMBER	
				5b. GRANT NUMBER	
				5c. PROGRAM ELEMENT NUMBER	
6. AUTHOR(S) David Wikner				5d. PROJECT NUMBER	
				5e. TASK NUMBER	
				5f. WORK UNIT NUMBER	
7. PERFORMING ORGANIZATION NAME(S) AND ADDRESS(ES) U.S. Army Research Laboratory ATTN: AMSRD ARL SE RM 2800 Powder Mill Road Adelphi, MD 20783-1197				8. PERFORMING ORGANIZATION REPORT NUMBER ARL-TR-4399	
9. SPONSORING/MONITORING AGENCY NAME(S) AND ADDRESS(ES)				10. SPONSOR/MONITOR'S ACRONYM(S)	
				11. SPONSOR/MONITOR'S REPORT NUMBER(S)	
12. DISTRIBUTION/AVAILABILITY STATEMENT Approved for public release; distribution unlimited.					
13. SUPPLEMENTARY NOTES					
14. ABSTRACT A one-week experiment was conducted to determine the millimeter-wave transmission loss due to dust. Transmission data was collected at 35, 94, and 217 GHz through a recirculating dust tunnel. Dust clouds of various densities were measured during the experiment. The millimeter-wave measurements were performed using transmitting sources on one side of the dust tunnel and antenna/detectors on the other. The hardware was designed to minimize noise and post-detection voltage drift. Even so, it was found that the transmission loss across the 1-m dust tunnel at high dust densities was lower than what could be measured accurately with the equipment. Therefore, the results given are limited to system noise and represent maximum transmission losses at the various frequencies. The results show losses less than 0.02 and 0.08 dB for 94 and 217 GHz respectively across one meter of dust with density 3000 mg/m ³ . The actual losses are lower but more sensitive instrumentation is required to determine the loss values precisely. Despite the limitations of the experiment, the data show that millimeter-wave imager performance will not be significantly impacted by even a very dense dust cloud.					
15. SUBJECT TERMS Millimeter wave, dust, propagation, helicopter brownout					
16. SECURITY CLASSIFICATION OF:			17. LIMITATION OF ABSTRACT UL	18. NUMBER OF PAGES 24	19a. NAME OF RESPONSIBLE PERSON David Wikner
a. REPORT U	b. ABSTRACT U	c. THIS PAGE U			19b. TELEPHONE NUMBER (Include area code) 301-394-0865

Contents

List of Figures	iv
List of Tables	iv
Acknowledgments	v
1. Introduction	1
1.1 Previous Measurements and Modeling	1
2. Experimental Procedure	3
3. Data Results and Analysis	8
4. Conclusion	12
5. References	13
Distribution List	14

List of Figures

Figure 1. Diagram of the MMW propagation experiment. Not drawn to scale. Shown are schematics of the 35, 94, and 217 GHz hardware. The transmitters were located on one side of the dust tunnel and the receivers on the other. The signal from the detectors was sent to video amplifiers and the data acquisition system (not shown).....	4
Figure 2. Transmitters are in the picture on the left and receivers are on the right. They are shown next to the MRI wind tunnel during the dust experiments. The glass windows have been replaced with low-loss polystyrene.....	5
Figure 3. Photograph looking down the length of the tunnel at 3218 mg/m^3 . The visibility is on the order of 3 meters. The polystyrene windows are seen on the right side of the image.....	7
Figure 4. Calibration plot for the 94 GHz propagation measurement system. The slope and y-intercept of the fit are shown on the plot.	9
Figure 5. Attenuation due to dust across a 1-m dust tunnel at 94 and 217 GHz after down-selecting data points with dust concentrations higher than 2000 mg/m^3 and noise lower than an acceptable threshold.	10
Figure 6. Worst case calculation of 94 GHz imager degradation due to a uniform high density dust cloud. Both the radar and radiometer are considered.	11

List of Tables

Table 1. A list of the data runs for the MMW propagation experiments. Dust density goals and measured values are shown in the last two columns.....	7
Table 2. Results from the 94 GHz transmission loss experiment.....	8
Table 3. Results from the 217 GHz transmission loss experiment.....	9

Acknowledgments

Thanks are given to Air Force Research Laboratory, Hanscom AFB, for assistance during the data collection and for generating software that enabled analysis of the data. Thanks are also due to the very capable and cooperative team at Midwest Research Institute, Kansas City, Missouri who ran the dust tunnel during the experiment and measured the dust properties. Thanks to Air Force Research Laboratory, Dayton, Ohio for program coordination and support. This work was sponsored by the DARPA Strategic Technology Office.

INTENTIONALLY LEFT BLANK

1. Introduction

Helicopters, when landing in dry, desert-type environments, create significant dust clouds that can obscure the pilot's vision. This situation, often referred to as brownout, is considered an emergency to the pilots involved and can result in a deadly accident. It is possible under brownout conditions that the pilot will become disoriented and lose control of the aircraft, collide with unseen obstacles, or land with lateral velocity, which can damage or roll the aircraft. A variety of technologies are being pursued to make brownout landings safer. These include LADAR, millimeter-wave (MMW) radar, and low-frequency RF bumpers. It is widely known that MMW signals have very low loss through fog, clouds, and most types of dust. What is not as well understood is how well MMW systems function through the very dense dust clouds generated by helicopters. The work described in this report helps answer that question.

We conducted an experiment to quantify the MMW signal propagation loss created by airborne, soil particulates. To conduct this experiment, a controlled dust storm with known density and particle size distribution was created in a recirculating dust tunnel. The MMW transmission loss across the width of the dust tunnel was measured at 35, 94, and 217 GHz using equipment designed and developed at the U.S. Army Research Laboratory. The densities and particle size distributions of the dust clouds created in the tunnel came close to duplicating actual dust cloud data collected at Yuma Proving Grounds on a variety of hovering, military helicopters. The results presented below help characterize these dust cloud losses, as is needed to predict MMW system performance in low visibility dust conditions. In the next section, previous measurements and modeling are discussed. This is followed by a description of the experiment, the results, and conclusions.

1.1 Previous Measurements and Modeling

Several studies have been conducted to measure and model the effects of dust storms at MMW frequencies (*1 through 4*). These efforts have often focused on frequencies around 40 GHz or lower for RF communications over long path lengths. Very limited data exist at higher frequencies. Due to the significant differences between dust clouds that interfere with RF communication and dust clouds generated by helicopters, data collected for RF communications at 40 GHz cannot be applied to the helicopter brownout situation. A communication link at 40 GHz has a wavelength that is significantly larger than the average dust particle size. This is because particles found in dust storms 20 to 100 meters above the ground, where communication antennas operate, are smaller than those picked up by helicopter rotors near the ground. Modeling the transmission loss of these dust clouds can be tricky. Published modeling results state that Rayleigh scattering approaches can be used with minimal error up to 300 GHz (*12*). However, the unusually large particle sizes found in helicopter-generated dust clouds, which were not considered in the model, would suggest that a full Mie scattering approach would be

more accurate. Although it is beyond the scope here, it will be the topic of a future paper. For the purposes of bounding the problem, presented below is a relatively simple method of predicting a minimum MMW transmission loss for a dust cloud based on the Rayleigh approximation.

MMW signal energy is lost in dust clouds through scattering, polarization loss, and absorption, all, of which are created when dust particles in a volume of air change the electromagnetic properties of that volume. The net effect of mixing air and dust particles can be described by a dielectric mixing model. Several mixing models have been applied to the dust problem including the Bruggeman formula (5) and the work by Looyenga (6). More recently, Karkkainen applied Finite Difference Time Domain methods to the problem and found a dependence on particle clustering in the effective permittivity of the mixture (7). It becomes apparent, after reviewing the models, that significant variation in the dust cloud permittivity results from the spatially-variant, physical properties of the dust cloud. These properties are difficult to measure experimentally. Alternatively, one can account for these unknowns by bounding the permittivity of the dust/air mixture as accurately as possible. The Hashin and Shtrikman bounds can be used for this purpose (8) and the validity of the method has been demonstrated by others (5). Bounding the problem in this way allows one to more easily make conservative system performance predictions without getting bogged down in the detailed spatial variability of the dust cloud. These bounds are described by

$$\begin{aligned}\mathcal{E}_{eff,\min} &= \mathcal{E}_e + \frac{f}{\frac{1}{\mathcal{E}_i - \mathcal{E}_e} + \frac{1-f}{3\mathcal{E}_e}} \\ \mathcal{E}_{eff,\max} &= \mathcal{E}_i + \frac{1-f}{\frac{1}{\mathcal{E}_e - \mathcal{E}_i} + \frac{f}{3\mathcal{E}_i}}\end{aligned}\tag{1}$$

where \mathcal{E}_i is the bulk permittivity of the dust, \mathcal{E}_e is the permittivity of the air, and f is the volume fraction of dust to air. It is assumed that $\mathcal{E}_e < \mathcal{E}_i$.

This Hashin/Shtrikman model requires knowledge of the bulk permittivity of the dust particles, which can be readily measured. Ansari and Evans (9), in surveying permittivity data from 10 to 37 GHz, found that both the real and imaginary parts of the bulk permittivity of dry soils are nearly frequency independent and that moisture content will increase these values dramatically, especially the imaginary part. A typical permittivity value of $2.515 + j0.074$ for dry sandy clay at 37 GHz is given in their article. It is also reported in (9) that the bulk permittivity of soil is almost unaffected by its chemical and mineral composition except where significant amounts of metallic or magnetic minerals are present.

Once the bounds of effective permittivity are determined for the dust cloud mixture, the attenuation can be calculated using the expression (10)

$$A(\lambda) = \frac{1.029 \times 10^6 \varepsilon''}{[(\varepsilon' + 2)^2 + \varepsilon''^2] \lambda} \sum_i N_i r_i \quad (\text{dB/km}) \quad (2)$$

where λ is the wavelength, ε' is the real part of the relative permittivity, ε'' is the complex part of the permittivity, N_i is the number of particles with radii between r_i and $r_i + \Delta r_i$ per m^3 . This equation is based on the Rayleigh approximation that relies on the wavelength being much larger than the dust particle sizes. As stated earlier, this provides a reasonable estimate for attenuation up to 300 GHz, albeit erring towards low attenuation. Determining a more precise value requires one to perform the Mie scattering calculations, but for many baseline MMW system design calculations the Rayleigh approach is sufficient and much simpler to implement.

Experimental measurements of dust clouds often use visibility as a measure of ground truth. Therefore, for the purposes of modeling, it is useful to have an expression that relates visibility to particle density and size. A precise relationship cannot be established for every case because one must assume an acceptable level of contrast between the object being viewed and the background. As reported in (10), experiments have been conducted to establish good approximations and the resulting expression relates dust particle density and particle radius to visibility as

$$V = \frac{5.51 \times 10^{-4}}{N_T r^2} \quad [\text{km}] \quad (3)$$

where N_T is the total number of particles per cubic meter and r is the average radius of the particles.

Equations 1 through 3 present a method of modeling the expected MMW attenuation from a dust cloud. The intent is to enable the reader to make baseline estimates of loss and to check the results of his/her own dust propagation experiments. In a later article the author intends to apply these equations and the MIE calculations to the data that follows. In the next sections the experiment and data are described in detail.

2. Experimental Procedure

The MMW dust propagation studies were carried out at a facility operated by Midwest Research Institute (MRI), Kansas City, MO. Prior to the dust tunnel testing, MRI quantified the dust density and particle size distribution of dust clouds created by a variety of hovering military helicopters. This carefully instrumented test, conducted at Yuma Proving Grounds, resulted in range and height profiles of the dust clouds as well as dust densities and particle sizes (11). The dust sampling equipment used in Yuma was placed near a variety of hovering helicopters. The distance of the dust samplers from the helicopters ranged from under the aircraft to about 50 meters away and their heights ranged from 0.5 to 7 m. The measured dust densities ranged from

150 to 3470 mg/m³ depending on aircraft type and sampler position. These results formed the basis for the dust tunnel experiments we conducted by defining the dust characteristics created in the tunnel. After several weeks of experimentation by MRI, using assorted dirt injection systems and recirculation methods, they were able to reliably create in the tunnel the conditions they had measured in the field.

The expectation going into the tunnel experiments was that the MMW propagation loss through the wind tunnel dust cloud would be on the order of 0.01 dB. This estimate was based on the 1-m width of the dust tunnel, the maximum expected dust density of about 3000 mg/m³, and modeled predictions (12). This meant that high sensitivity was required in the instrumentation to characterize the propagation loss. We determined that we could achieve this level of sensitivity using a simple transmitter/receiver setup, if the issues of transmitter and receiver drift were considered in the design. This was done for 35, 94, and 217 GHz. The transmitter and receiver layouts are shown in figure 1.

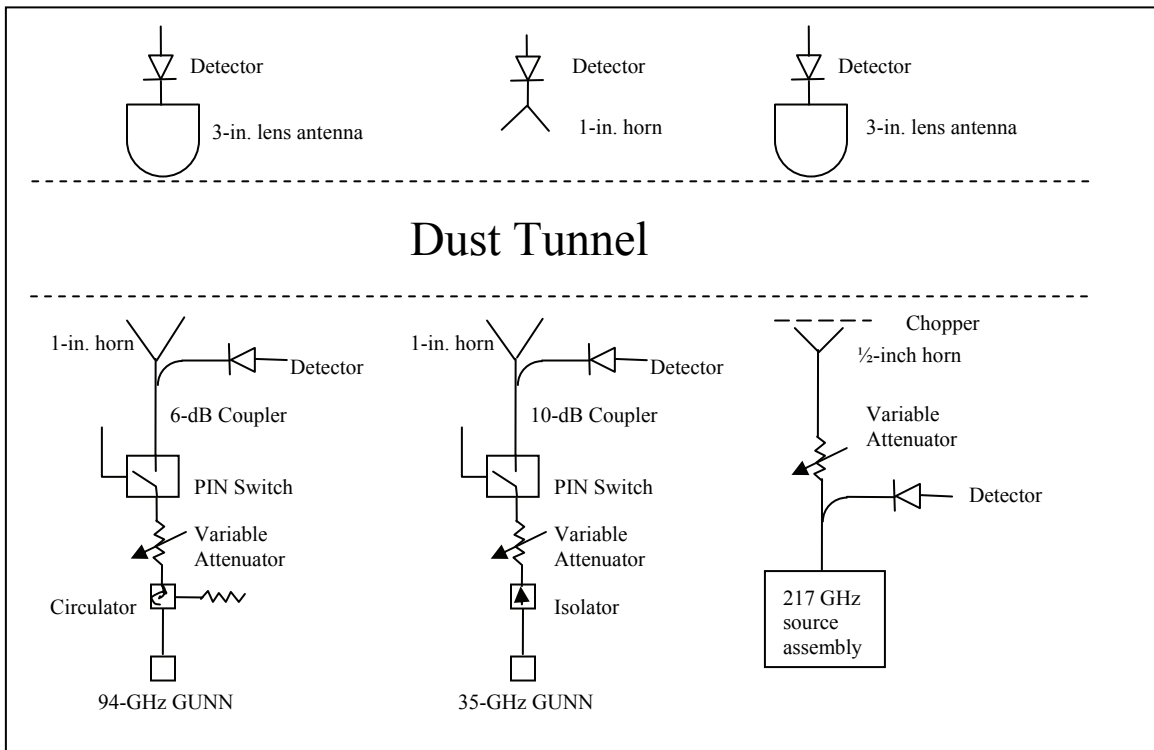


Figure 1. Diagram of the MMW propagation experiment. Not drawn to scale. Shown are schematics of the 35, 94, and 217 GHz hardware. The transmitters were located on one side of the dust tunnel and the receivers on the other. The signal from the detectors was sent to video amplifiers and the data acquisition system (not shown).

The 94 and 35 GHz circuits have essentially the same design. Each is driven by a GUNN source followed by a variable attenuator, PIN switch, coupler, and antenna. The 94 and 35 GHz sources have powers at the transmit antennas of 6 mW and 43 mW, respectively. The variable attenuators are precise to 0.01 dB and are used to check the linearity of the detector circuit and

calibrate the system. The PIN switch is used to turn the transmitter on and off at about 1 kHz. This square-wave modulates the transmitted signal and synchronous detection is used to remove fluctuations in the video amplifier circuit that follows the detector. A portion of the transmitter signal is coupled off to a power detector to track changes in signal amplitude. This information can be used to correct the receiver data for large changes during a measurement. We demonstrated in the lab that the combination of the synchronous detection and the transmitter monitor provided the 0.01 dB of accuracy required to measure propagation loss in the dust tunnel. The 217 GHz system is similar in design with a couple of exceptions. A 217 GHz PIN switch was not available so a mechanical chopper is used instead. The chopping rate was 100 Hz at 217 GHz. Also, the 217 GHz source is not a GUNN. It is an assembly built by Virginia Diodes that uses a Dielectric Resonator Oscillator (DRO) and 4 doublers to generate 5 mW at 217 GHz. The receiver antennas were selected to produce a signal level in the square-law region of the detectors (around -20 dBm). This yields an output voltage that is linearly proportional to input RF power and maximizes sensitivity (dV/dP).

The MRI dust tunnel has windows located on its sides so that instruments can be set up to measure propagation through the dust. These windows are made of reinforced glass and we found that the loss through each pane of glass was 5 dB at 94 GHz. This was deemed too large so we made polystyrene windows to replace the glass. The ½-in. thick polystyrene windows each have a measured loss of about 0.01 dB and did not accumulate a significant amount of dust during the experiment. The transmitters and receivers are shown in figure 2 during data collection at the MRI wind tunnel.

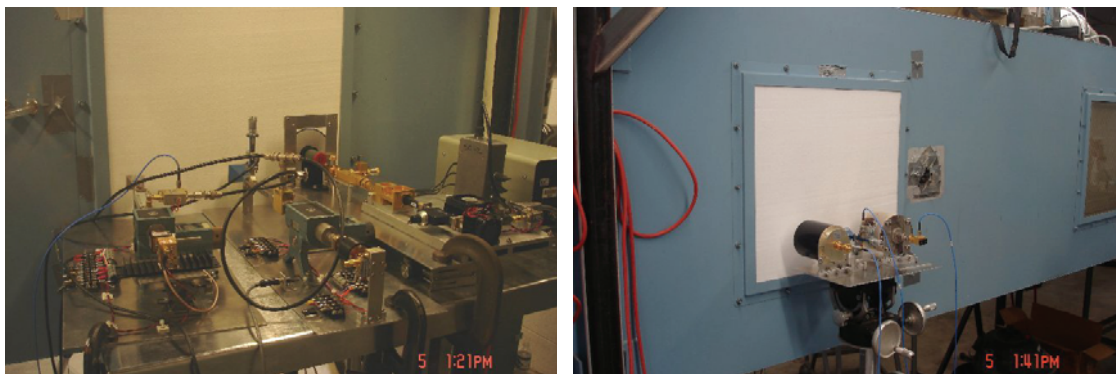


Figure 2. Transmitters are in the picture on the left and receivers are on the right. They are shown next to the MRI wind tunnel during the dust experiments. The glass windows have been replaced with low-loss polystyrene.

The MMW dust propagation experiments were conducted over a period of one week. During that week, propagation loss was measured at a variety of dust densities using the equipment described above. For each data run there was a target dust density. After the tunnel was turned on and the dirt injected, a few minutes were required to reach a somewhat uniform distribution of dust in the tunnel. After this was accomplished, an MMW propagation measurement was made and the dust was sampled by MRI personnel using equipment that collects a known volume of air

from the tunnel. Soon after, the run ended and the tunnel was turned off. MRI then took the sampled dust to a nearby laboratory to determine the density and particle size distribution that was actually achieved. Table 1 shows a portion of the data collected by MRI for each of the dust runs on which we collected data. Of the 23 data runs, most had a target of 3000 mg/m³. This target was based upon an earlier field test conducted by MRI in the desert with actual hovering helicopters. It represents a typical maximum density measured during the testing. In many cases the dust density achieved in the tunnel was within $\pm 10\%$ of the target. The particle size distribution goal for the runs was 23% for particles < 75 μm , 25% for particles 75 to 150 μm , 22% for particles 150 to 420 μm , and 30% for particles >420 μm . The actual dust clouds at this density often had 10 to 20% too much of the small particles and 10 to 20% too little of the large particles. The medium sized particles were often within a few percent. Figure 3 shows a photograph of the inside of the dust tunnel at a density of 3218 mg/m³. The photo was taken looking down the length of the tunnel and shows a visibility on the order of 3 meters.

The stability of the MMW equipment was important for a good measurement. As mentioned previously, synchronous detection and transmitter power monitoring were used to reduce system noise as much as possible. Additional accuracy was achieved by making a comparative measurement between clear air and dusty air. We collected clear air propagation data just a few minutes before dust data. Comparing these two values gives a measure of propagation loss while minimizing the drift of the system, which becomes larger over time.

Data was also averaged to reduce the measured noise. During a typical dust run 5 – 6 data points were collected, each separated in time by 15 seconds, with each data point representing 10,000 A-to-D samples for a total of 0.15 seconds of integration time per data point. The data points were averaged for a total integration time of 0.75 seconds. This process of integration reduces the measured noise by 23 dB. Erroneous changes in the detector signal can still be seen after this integration and are primarily due to system drift and must be removed after data collection.

It was determined midway through the data collection that the loss due to dust at 35 GHz was extremely low. So low, in fact, that we were spending an inordinate amount of time trying to pull a signal out of the noise. For this reason we made the decision to abandon the 35 GHz measurements and focus on getting good results at 94 and 217 GHz.

Table 1. A list of the data runs for the MMW propagation experiments. Dust density goals and measured values are shown in the last two columns.

	Date	Temperature °F	% Relative Humidity	Target Concentration mg/m³	Average Concentration mg/m³
Test DA-315	6/5/2006	72.4	58.4	3,000	3,379
Test DA-316	6/5/2006	73.4	54.3	3,000	3,218
Test DA-317	6/6/2006	71.8	65.3	250	170
Test DA-318	6/6/2006	71.8	61.7	500	284
Test DA-319	6/6/2006	73	60.2	1,000	1,180
Test DA-320	6/6/2006	77	56.1	2,000	2,024
Test DA-321	6/6/2006	76	55.6	3,000	2,673
Test DA-322	6/6/2006	76.2	61.2	3,000	3,002
Test DA-323	6/7/2006	68.4	67.1	3,000	3,127
Test DA-324	6/7/2006	71	51.6	3,000	2,935
Test DA- 325	6/7/2006	73.6	45.7	3,000	3,207
Test DA-326	6/7/2006	75.2	46.1	3,000	2,329
Test DA-327	6/7/2006	76.6	43.1	3,000	2,802
Test DA-328	6/7/2006	76.2	44.5	n/a	1,066
Test DA-329	6/8/2006	70.2	56.9	n/a	488
Test DA-330	6/8/2006	71.6	53.2	n/a	561
Test DA-331	6/8/2006	76.2	49.8	3,000	2,889
Test DA-332	6/8/2006	78.3	47.8	1,500	1,288
Test DA- 333	6/8/2006	79.1	47.2	1,200	1,226
Test DA-334	6/8/2006	79.2	47.3	1,200	1,237
Test DA-335	6/9/2006	68.7	61.8	2,000	2,254
Test DA-336	6/9/2006	71.8	55.6	1,000	1,008
Test DA-337	6/9/2006	75.6	53.4	2,000	2,616



Figure 3. Photograph looking down the length of the tunnel at 3218 mg/m³. The visibility is on the order of 3 meters. The polystyrene windows are seen on the right side of the image.

3. Data Results and Analysis

As stated in the previous section, propagation measurements were made through a clear air condition in the wind tunnel and then shortly after in a dust condition. The two values were compared to determine the change in detected signal due to dust. The results for 94 and 217 GHz are shown in tables 2 and 3, respectively. For each data run, the dust density and detected change in RF power are given. Negative values of change indicate a decrease in RF signal in the presence of dust. It can be seen that in some cases the change is positive, which indicates an increase in signal in the presence of dust. This is an indication of system noise or drift. During the week of measurements, various sources of noise were discovered and methods were developed to remove them. Two simple changes made during the experiment involved correcting a bad ground and adjusting the frequency of the RF signal modulation. The RF modulation frequency of the 94 GHz channel was increased from 100 Hz to 1000 Hz to reduce 1/f noise. The 217 GHz channel was limited to 100 Hz by the mechanical chopper. The primary source of measurement noise that remained was caused by drift in the video amplifier gain after the RF detectors. There were about 3 to 5 minutes between a clear air measurement and a dust measurement. It was discovered late in the week that the MRI dust sampling equipment may have caused the video amplifier drift. The fans used to draw dust into the cyclone dust samplers blew a significant amount of air across the video amplifier circuits during a dust run. They were located about 8 feet from the amplifiers, but there was enough air movement to affect the temperature of the amplifiers. We found a way to deflect this air and improved the amplifier stability.

Table 2. Results from the 94 GHz transmission loss experiment.

Run #	Density (mg/m ³)	Detected Change in 94 GHz Power (dB)
DA-315	3379	-0.11 +/- 0.1
DA-316	3218	-0.02 +/- 0.02
DA-317	170	-0.14 +/- 0.08
DA-318	284	-0.3 +/- 0.1
DA-319	1180	0.03 +/- 0.12
DA-320	2024	-0.06 +/- 0.14
DA-321	2673	-0.01 +/- 0.11
DA-322	3002	-0.1 +/- 0.08
DA-324	3127	-0.2 +/- 0.02
DA-331	2889	0.002 +/- 0.11
DA-332	1288	-0.13 +/- 0.02
DA-334	1237	-0.31 +/- 0.06
DA-335	2254	-0.02 +/- 0.03
DA-336	1008	-0.01 +/- 0.02
DA-337	2616	0.01 +/- 0.02

Table 3. Results from the 217 GHz transmission loss experiment.

Run #	Density (mg/m ³)	Detected Change in 217 GHz Power(dB)
DA-315	3379	-0.35 +/- 0.2
DA-316	3218	0.16 +/- 0.1
DA-317	170	-0.4 +/- 0.14
DA-318	284	0.46 +/- 0.17
DA-319	1180	-0.08 +/- 0.18
DA-320	2024	0.1 +/- 0.27
DA-321	2673	-0.13 +/- 0.22
DA-322	3002	0.004 +/- 0.08
DA-324	3127	0.01 +/- 0.17
DA-331	2889	-0.11 +/- 0.08
DA-332	1288	-0.26 +/- 0.05
DA-335	2254	0.22 +/- 0.16
DA-336	1008	-0.12 +/- 0.03
DA-337	2616	-0.09 +/- 0.09

It was important to establish a good calibration of the 35, 94, and 217 GHz instrumentation to properly interpret the data. This was accomplished by collecting calibration data regularly under clear air wind tunnel conditions using the precision attenuator in each transmitter circuit. Data was taken as the attenuator was changed over a fixed attenuation range. Figure 4 shows the results of the calibration for the 94 GHz system. Note the reasonably good linearity of the results which indicates that we were in the “square law” region of the detectors, where RF power is linearly proportional to output voltage. This is also the region in which voltage sensitivity, or dV/dP , is maximized. An inspection of the plot indicates that we have a slope of -0.17896 V/dB, or about 2 mV/0.01 dB. This is well above the 50 micro-volt quantization limit of the A-to-D.

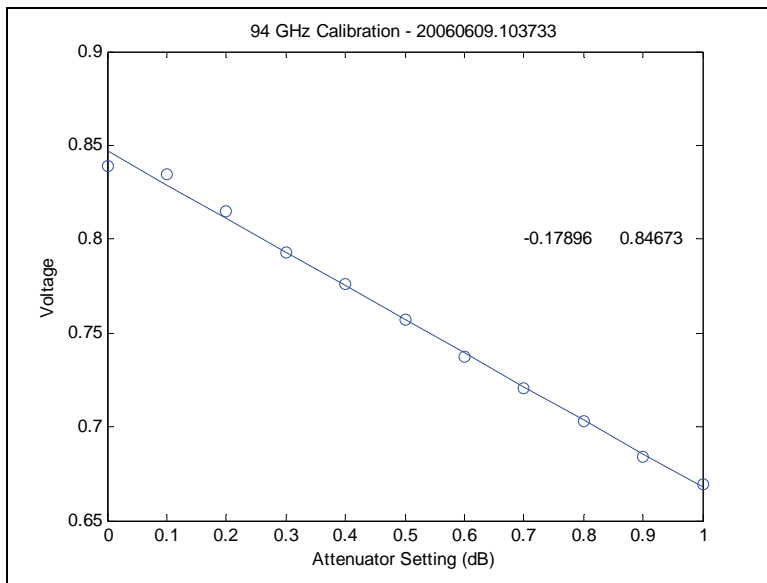


Figure 4. Calibration plot for the 94 GHz propagation measurement system. The slope and y-intercept of the fit are shown on the plot.

Interpreting the wind tunnel results is an exercise in error analysis. We want both low standard deviation in a given measurement and low system drift between the clear air and dust measurements. It is clear from table 3, for example, that there is no measureable change in power with dust density. For example, run 317 had the lowest dust density but showed one of the highest power changes for both 94 and 217 GHz. These results can be considered erroneous due to excessive system drift. It is safe to say that the measurement equipment did not have the precision to distinguish variations in dust density. Further, the variability in the performance of the equipment makes many of the data points questionable. So, we must filter the results to draw any conclusion at all. We eliminate from consideration any data run with a dust density less than 2000 mg/m³ and power difference standard deviation greater than 0.03 dB for 94GHz and 0.1 dB for 217 GHz. What are left are the values shown in figure 5. Although the number of data points is limited, we can see trends in the data. At 94 GHz the average change in power is about 0.025 dB over 1 meter of dust. This ignores the 0.2 dB data point that appears to be an outlier and due to a receiver drift between the clear air and dust measurements. At 217 GHz, the average attenuation per meter is about 0.1 dB. This is consistent with our expectation that the 217 GHz attenuation would be a bit higher than 94 GHz. The larger error bars at 217 GHz show, however, that this receiver was noisy and we can't really state with confidence a value to better than ±0.1 dB.

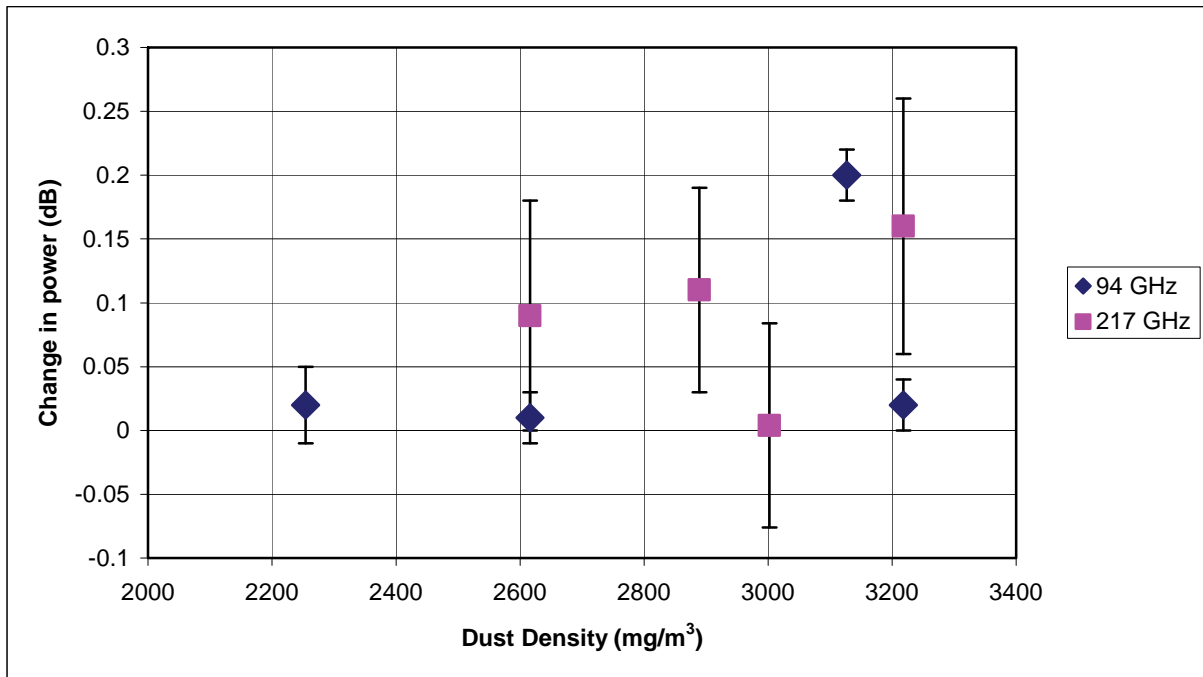


Figure 5. Attenuation due to dust across a 1-m dust tunnel at 94 and 217 GHz after down-selecting data points with dust concentrations higher than 2000 mg/m³ and noise lower than an acceptable threshold.

The data show that system noise was the limiting factor during the test. Even so, the data allow us to put an upper bound on transmission loss due to dust at these frequencies. We can calculate a worst case value for propagation through a simulated dust cloud. Referring to the drawing in figure 6, imagine a hemispherical dust cloud with a radius of 30 m. We can assume as a worst case that the entire dust cloud has a density of 3218 g/m^3 (from run 316). If a sensor is located just outside the dust cloud and is pointed at its center, we can calculate the maximum reduction in scene contrast due to dust. For a radar, the maximum 2-way loss due to the dust is just the attenuation per meter times the number of meters in the 2-way path. For 94 GHz, using the data from figure 5, this is 0.02 dB times 60 meters or 1.2 dB. On the other hand, for an imaging radiometer the reduction in contrast created by the dust cloud is due to two things. The dust cloud increases the brightness temperature of the sky illuminating the scene and attenuates the resulting reflected and emitted signal on the path to the sensor. Take, for example, a metal plate that reflects 100 K zenith sky radiation towards the radiometer. Assume that the ground and ambient temperature are 300 K. Assume the contrast between the plate and the ground in the absence of dust is 200 K. The emitted sky energy has a transmission of 0.76 (1.2 dB of loss). Further, the sand cloud emits a brightness temperature equal to $300 \text{ K} * (1 - 0.76) = 72 \text{ K}$. Therefore, the plate brightness temperature scene at the radiometer is $(100 \text{ K} * 0.76) + 72 \text{ K} = 148 \text{ K}$. The scene contrast is now $300 \text{ K} - 148 \text{ K} = 152 \text{ K}$, a reduction of 24% or about 1 dB. This is a measurable reduction in contrast, but not one that will significantly degrade image quality.

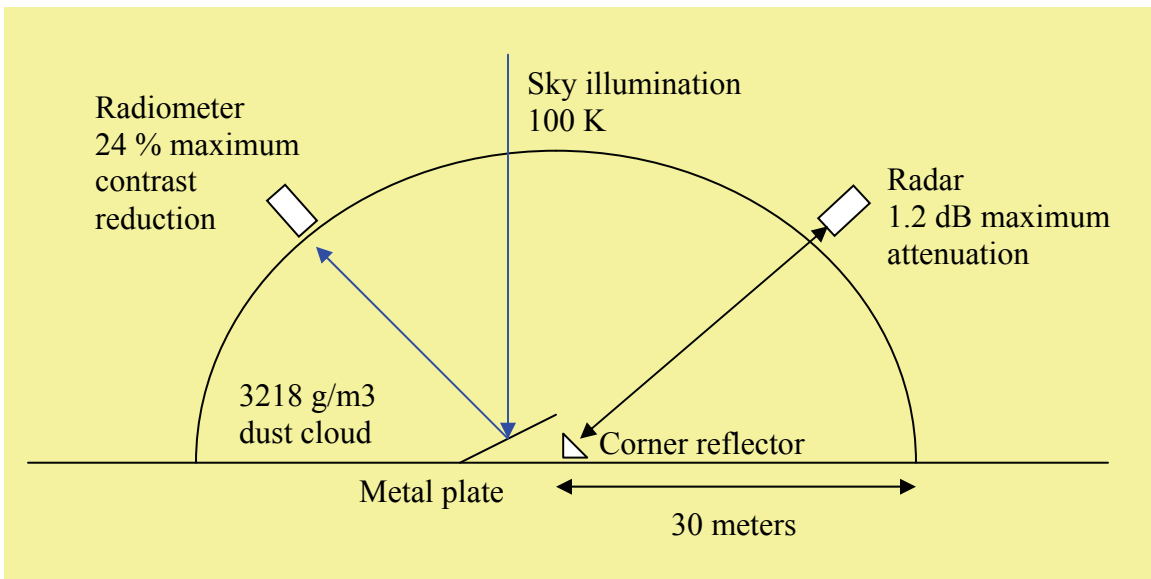


Figure 6. Worst case calculation of 94 GHz imager degradation due to a uniform high density dust cloud. Both the radar and radiometer are considered.

4. Conclusion

It is clear from this experiment that the transmission loss at 94 and 217 GHz is very low over a 1-m path. So low, in fact, that measuring the exact loss using a simple propagation technique is very challenging. Using results that had acceptable noise levels and dust concentrations between 2000 and 3200 mg/m³, the experiment gives us an upper bound on the transmission loss of a of 0.02 dB/m for 94 GHz and 0.1 dB/m at 217 GHz. The 35-GHz loss was too small to measure, but from modeled results, we can assume that it is lower than the loss at 94 GHz.

Some theoretical models suggest that the exact losses and extinction coefficients at these frequencies may be considerably lower than the maximums given here. A model presented in Brussaard (*13*) indicates that attenuation may be as low as 0.001 dB/m at 94 GHz for 10-m visibility dust. To make an accurate determination of this value experimentally requires more precise hardware; an interferometer might provide the sensitivity required to measure the exact loss over 1 m. This experiment is not without issues though. Building an interferometer with a 1-m baseline and 0.1 mm precision will be an engineering challenge. One must also consider the effect of the vibrating wind tunnel in the midst of the interferometer and what effect it might have on the measurement accuracy.

Even without determining the exact loss, this experiment has provided upper bounds that enable us to determine a conservative estimate of the performance of a MMW sensor in an actual dust cloud. The calculations show that the loss through a high density (3-m visibility or 3000 mg/m³ density) 30-m dust cloud would reduce the 94 GHz signal level by at most 1.2 dB in a two-way radar signal path and about 24% for MMW radiometer. These losses would likely have small effects on imager performance during a helicopter landing. The actual losses are most likely lower than measured here, which implies that even smaller effects on imaging will actually be seen.

5. References

1. Abdulla, S.A.A.; Al-Rizzo, H. M.; Cyril, M. M. Particle-Size Distribution of Iraqi Sand and Dust Storms and their Influence on Microwave Communication Systems. *IEEE Trans. on Antennas and Propagation* **Jan. 1988**, 36, (1), 114–126.
2. Vishvakarma, B. R.; Rai, C. S. Limitations of Rayleigh scattering in the prediction of millimeter wave attenuation in sand and dust storms. *Geoscience and Remote Sensing Symposium, 1993, IGARSS '93, Better Understanding of Earth Environment* **Aug. 1993**, 1 (18-21), 267–269.
3. Ali, A. A.; Alhaider, M. A. Millimeter-wave Propagation in Arid Land – A Field Study in Riyadh. *IEEE Trans. on Antennas and Propagation* **May 1992**, 40 (5), 492–499.
4. Afzaal, K.; Bandopadhyaya, T. K.; Poonam, S. Effect of soil textural class and relative humidity of regions in accurate prediction of attenuation of millimeter waves during sand and dust storms. *Physics and Engineering of Millimeter and Sub-Millimeter Waves*, 2001. The Fourth International Kharkov Symposium 4–9 June 2001, 1, 393–395.
5. Karkkainen, K.; Sihvola, A.; Nikoskinen, K. Effective Permittivity of Mixtures: Numerical Validation by the FDTD Method. *IEEE Trans. Geoscience and Remote Sensing* **May 2000**, 38 (3).
6. Looyenga, H. Dielectric constants of mixtures. *Physica* **1965**, 31, 401–406.
7. Karkkainen, K.; Sihvola, A.; Nikoskinen, K. Analysis of a Three-Dimensional Dielectric Mixture with Finite Difference Method. *IEEE Trans. Geoscience and Remote Sensing* **May 2001**, 39 (5).
8. Hashin, Z.; Shtrikman, S. A Variational Approach to the Theory of Effective Permeability of Multiphase Materials. *Journal of Applied Physics* **Oct. 1962**, 33 (10).
9. Ansari, A.; Evans, B. G. Microwave propagation in sand and dust storms. *IEE Proc.* **Oct. 1982**, 129 (Pt. F, No. 5).
10. Goldhirsh, J. A Parameter Review and Assessment of Attenuation and Backscatter Properties Associated with Dust Storms over Desert Regions in the Frequency Range of 1 to 10 GHz. *IEEE Trans. A&P* **November 1982**, AP-30 (6), 1121–1127.
11. Internal documentation of Midwest Research Institute, POC: Chat Cowherd.
12. Brussaard, G.; Watson, P. A. *Atmospheric Modeling and Millimetre Wave Propagation*; published by Chapman & Hall, 1995.

Distribution List

<u>NO.</u> <u>COPIES</u>	<u>ORGANIZATION</u>	<u>NO.</u> <u>COPIES</u>	<u>ORGANIZATION</u>
1 PDF	ADMNSTR DEFNS TECHL INFO CTR ATTN DTIC OCP (ELECTRONIC COPY) 8725 JOHN J KINGMAN RD STE 0944 FT BELVOIR VA 22060-6218	1	PM TIMS, PROFILER (MMS-P) AN/TMQ-52 ATTN B GRIFFIES BUILDING 563 FT MONMOUTH NJ 07703
2	DARPA ATTN IXO S WELBY ATTN STO D TOURNEAR 3701 N FAIRFAX DR ARLINGTON VA 22203-1714	1	US ARMY AVIATION AND MISSILE CMND PROJECT MANAGER UTILITY HELICOPTERS ATTN AMSAM DSA UH BLDG 5308 REDSTONE ARSENAL AL 35898-5208
1	OFC OF THE SECY OF DEFNS ATTN ODDRE (R&AT) THE PENTAGON WASHINGTON DC 20301-3080	1	SMC/GPA 2420 VELA WAY STE 1866 EL SEGUNDO CA 90245-4659
1	US ARMY RSRCH DEV AND ENGRG CMND ARMAMENT RSRCH DEV AND ENGRG CTR ARMAMENT ENGRG AND TECHNLGY CTR ATTN AMSRD AAR AEF T J MATTS BLDG 305 ABERDEEN PROVING GROUND MD 21005-5001	1	US ARMY INFO SYS ENGRG CMND ATTN AMSEL IE TD F JENIA FT HUACHUCA AZ 85613-5300
1	US ARMY TRADOC BATTLE LAB INTEGRATION & TECHL DIRCTRT ATTN ATCD B 10 WHISTLER LANE FT MONROE VA 23651-5850	1	US ARMY PROGRAM EXECUTIVE OFC - AVIATION ATTN L MERRITT 5681 MILLS RD REDSTONE ARSENAL AL 35898
2	US ARMY RSRCH DEV AND ENGRG CTR COMM & ELECTRNCS RSRCH DEV & ENGRD CNTR NIGHT VISION & ELECTRNC SENS DIRECTORATE ATTN A TRAN ATTN T BUI 10221 BURBECK RD BLDG 305 FT BELVOIR VA 22060-5806	1	COMMANDER US ARMY RDECOM ATTN AMSRD AMR W C MCCORKLE 5400 FOWLER RD REDSTONE ARSENAL AL 35898-5000
		1	US ARMY RSRCH DEV AND ENGRD CMND AVIATION & MISSILE RSRCH DEV & ENGRD CTR ATTN AMSRD AMR AS CC L LEVITT BLDG 5400 REDSTONE ARSENAL AL 35898-5000

<u>NO.</u>	<u>COPIES</u>	<u>ORGANIZATION</u>
1		US ARMY RSRCH DEV AND ENGRG CMND AVIATION APPLIED TECH DIRECTORATE ATTN AMSRD AMR AA I M WALSH 401 LEE BLVD FT EUSTIS VA 23604
1		US ARMY RSRCH LAB ATTN AMSRD ARL CI OK TP TECHL LIB T LANDFRIED BLDG 4600 ABERDEEN PROVING GROUND MD 21005-5066
1		US AIR FORCE RSRCH LAB ATTN AFRL/SNZC W HARRINGTON 2241 AVIONICS CIR BLDG 620 WRIGHT PATTERSON AFB OH 45433-7303
1		US GOVERNMENT PRINT OFF DEPOSITORY RECEIVING SECTION ATTN MAIL STOP IDAD J TATE 732 NORTH CAPITOL ST NW WASHINGTON DC 20402
1		DIRECTOR US ARMY RSRCH LAB ATTN AMSRD ARL RO EV W D BACH PO BOX 12211 RESEARCH TRIANGLE PARK NC 27709
6		US ARMY RSRCH LAB ATTN AMSRD ARL CI OK T TECHL PUB ATTN AMSRD ARL CI OK TL TECHL LIB ATTN AMSRD ARL SE RM D WIKNER ATTN AMSRD ARL SE RM E ADLER ATTN AMSRD ARL SE RM J SILVIOUS ATTN IMNE ALC IMS MAIL & RECORDS MGMT ADELPHI MD 20783-1197

INTENTIONALLY LEFT BLANK.